JOVIAN DECAMETRIC IO–RELATED SOURCE AND INTERPLANETARY SCINTILLATION

K. Maeda*

Abstract

We analyzed two–frequency observations of Jovian decametric Io–related radiation to measure the rate of the frequency drift due to the combined effect of the emission source structure and interplanetary scintillation (IPS). The frequency drift rates were estimated by a cross–correlation analysis of the IPS intensity fluctuations at the two frequencies. It is concluded that the IPS frequency drift rate in the Io–related source A (Io–A) storm changes systematically as a function of elongation from the sun. The magnitude of the frequency drift rate at an elongation of 90° is about 5 MHz sec^{-1} at frequencies near 22–23 MHz. The result for an Io–related source B (Io–B) storm indicates that the sense of the IPS frequency drift in the Io–B storm is opposite to that in the Io–A storm.

1 Introduction

The probability of occurrence of Jovian decametric storm activity within a given narrow frequency range is a function of the System III central meridian longitude (CML) and the orbital phase angle of the innermost Galilean satellite Io measured from its superior geocentric conjunction (Io phase). There are well–defined zones of CML within which the occurrence probability of the Jovian storm activity is relatively high. According to the classification in Table 4 of Carr et al. [1983], they are called sources A, B, and C. Each source consists of Io–related and Io–unrelated components. The Io–related source B (Io–B) emission occurs only when the Io phase is in the vicinity of 90°, and Io–related source A (Io–A) and Io–related source C (Io–C) emission when the phase is near 240° (more or less). Such emission anisotropy has long been interpreted as evidence of the beaming of Jovian decametric radiation.

It is well known that when the Jovian decametric radiation is received on Earth, it exhibits, in addition to a relatively slow intrinsic burst structure, strong and more rapid intensity fluctuations of the order of seconds (so–called L bursts). Such intensity fluctuations are due mainly to diffraction by electron density irregularities in the solar wind moving across the line of sight, i.e., interplanetary scintillation (IPS) [Douglas and Smith, 1967;

*Department of Physics, Hyogo College of Medicine Nishinomiya, Hyogo 663, Japan

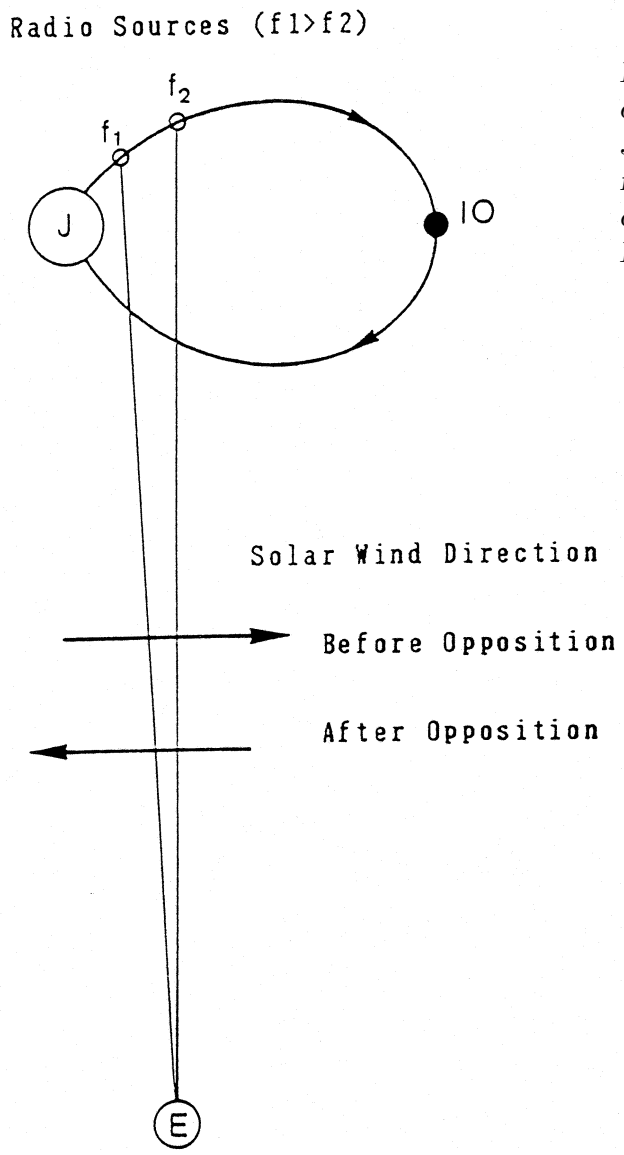

Figure 1: Schematic showing of the IPS geometry for the Io–A storm observation. E, and J indicate Earth, and Jupiter, respectively. It is assumed that the sources at the two frequencies (f1 and f2, f1>f2) are located in the Io–excited flux tube.

Slee and Higgins, 1968; Genova and Leblanc, 1981; Maeda, 1981]. More rapid spikes of the order of milliseconds (so–called S bursts) are sometimes observed in the Io–related storm, particularly in the Io–B storm.

It is widely believed that the emission frequency of Jovian decametric radiation is close to the electron cyclotron frequency at the emission point (see, for example, Goldstein and Goertz [1983]). For the Io–related sources a given radiating magnetic flux tube is excited by the orbital motion of Io. In the Io–excited flux tube the sources at different frequencies are distributed along the flux tube. Since the magnetic field strength in the flux tube increases with decreasing altitude, the higher frequency source is located closer to the planet than the lower frequency one (refer to Figure 1).

Genova and Boischot [1981] proposed to test such an Io–related source structure using the IPS phenomenon. The difference in the apparent source positions (i.e., projected on the sky) causes a displacement of the IPS diffraction pattern on the ground at one frequency with respect to that at another frequency. If two frequencies are close enough,

the diffraction patterns of the two frequencies would be correlated. Since the IPS intensity fluctuations are caused by the drift of the diffraction pattern due to the solar wind motion radially outward from the sun, the intensity fluctuation peaks at one frequency are temporally displaced with respect to the corresponding ones at another frequency. Genova and Boischot were apparently the first to indicate that a frequency drift component due to this effect of the solar wind motion should be discernible in dynamic spectra. They investigated the Nancay dynamic spectra, and found the frequency drift pattern, the frequency drift sense being consistent with that inferred from their idea. Boischot et al. [1987] confirmed the result of Genova and Boischot by more extensive analysis of the dynamic spectral data, including Io–unrelated storm components. However, the results from the analysis of the dynamic spectrum were qualitative. It is necessary to confirm their results by a more quantitative analysis. We present the first accurate measurements of the IPS frequency drift rate based on two–frequency observations.

2 Geometry of the IPS observation

Figure 1 schematically shows the geometry of the two–frequency IPS observation for the Io–A storm. Since the Io phase is near 240°, Io is located on the west side of the planet in the sky as viewed from Earth, and in the Io–excited flux tube the higher frequency (f1) source is on the east side of the lower frequency (f2) one. Since the right hand circular component is dominant in the Io–A emission, it is assumed in Figure 1 that the sources are located in the northern foot of the Io–excited flux tube. As indicated in Figure 1, the solar wind flows westward across the line of sight before opposition. The electron density irregularities in the solar wind move across the line of sight to the higher frequency source first, and then across the line of sight to the lower frequency one. As a result, the same IPS intensity fluctuation peaks are observed at the higher frequency first, then at the lower frequency (i.e., negative frequency drift). Since after opposition the flow direction of the solar wind reverses, the sense of the frequency drift would change to positive. It is therefore expected that for the Io–A storm the frequency drift due to the solar wind will be negative before opposition and positive after opposition.

The IPS geometry for the Io–B storm can also be discussed in a similar manner as for the Io–A storm, taking into account the difference in Io's orbital position. Since the Io phase is near 90° for the Io–B storm, Io is on the east side of the planet. The higher frequency source is therefore located on the west side of the lower frequency one. It is therefore expected that the sense of the IPS frequency drift is opposite to that of the Io–A storm.

3 Observations

Observations were made over two apparitions of Jupiter (1988–1990), using an 8–element right–hand conical log–spiral array [Maeda, 1987]. The output of the array was divided into two components, one for fixed–frequency observations and the other for the dynamic spectral observations. The dynamic spectral observations were made using a spectrum analyzer (a kind of spectrograph) and a facsimile recorder. We used the dynamic spectral

data just for the monitoring of the Jovian decametric storm, but not for a detailed analysis. The fixed–frequency observations were made at two frequencies between 21.8 and 23.3 MHz. The observation frequencies were sometimes changed to avoid man–made interference. Two commercial communications receivers, each having a bandwidth of about 10 kHz, were used. The audio frequency outputs of the receivers were recorded on a two–channel digital audio tape recorder. Our observations were focused on the Io–A and Io–B storms, because they are well–predictable and strong enough to obtain the data with a high signal–to–noise ratio.

4 Analysis

The replayed audio frequency output signal was detected and converted to the intensity fluctuations. The intensity fluctuations at each frequency were digitized every 20 or 50 msec. The longer sampling time was used for the storms that occurred close to opposition, because the average time scale of the IPS fluctuations becomes longer near opposition (see for example, Maeda [1981]).

For each storm we selected the data segments in each of which we could clearly see the IPS fluctuations at both frequencies. Each selected data segment consisted of 200–400 data points, i.e., 4–20 sec long. The cross–correlation analysis was made for each pair of the selected data segments. Figure 2 indicates how we did the cross–correlation analysis. In Figure 2a the observed intensity fluctuation curves (after digitization) at the two frequencies are displayed. In each data segment, indicated by the arrows, four prominent IPS fluctuation peaks are seen. The calculated cross–correlation curve of these data segments is indicated in Figure 2b. We estimated the delay time at which the peak correlation occurred for each data–segment pair, as indicated by t(peak) in Figure 2b, and referred it to the delay time for the data–segment pair. Then we investigated the distribution of the estimated delay times for a given storm, using only the data–segment pairs which had a peak correlation value greater than 0.5.

5 Results

In this analysis we used the elongation, ϵ, that was measured clockwise from 0° to 360° as shown in Figure 3. Figure 4 indicates the delay time distribution diagrams for 5 Io–A storms observed at different elongations. In Figure 4 the delay time of the lower frequency curve with respect to the higher frequency one is used. The positive delay time therefore means that the intensity fluctuation curve at the lower frequency follows that at the higher frequency (i.e., the negative frequency drift). Figures 4a and 4b indicate that the negative frequency drift was dominant before opposition ($\epsilon < 180°$). On the other hand, Figures 4d and 4e indicate that the sense of the IPS frequency drift changed to positive after opposition ($\epsilon > 180°$). It is interesting to note that in Figure 4c the negative frequency drift was still dominant, although the November 29 Io–A storm occurred just after opposition ($\epsilon = 187°$). This apparently indicates that the orbital motion of Earth becomes relatively important near opposition. On November 29, 1988, the speed of drift

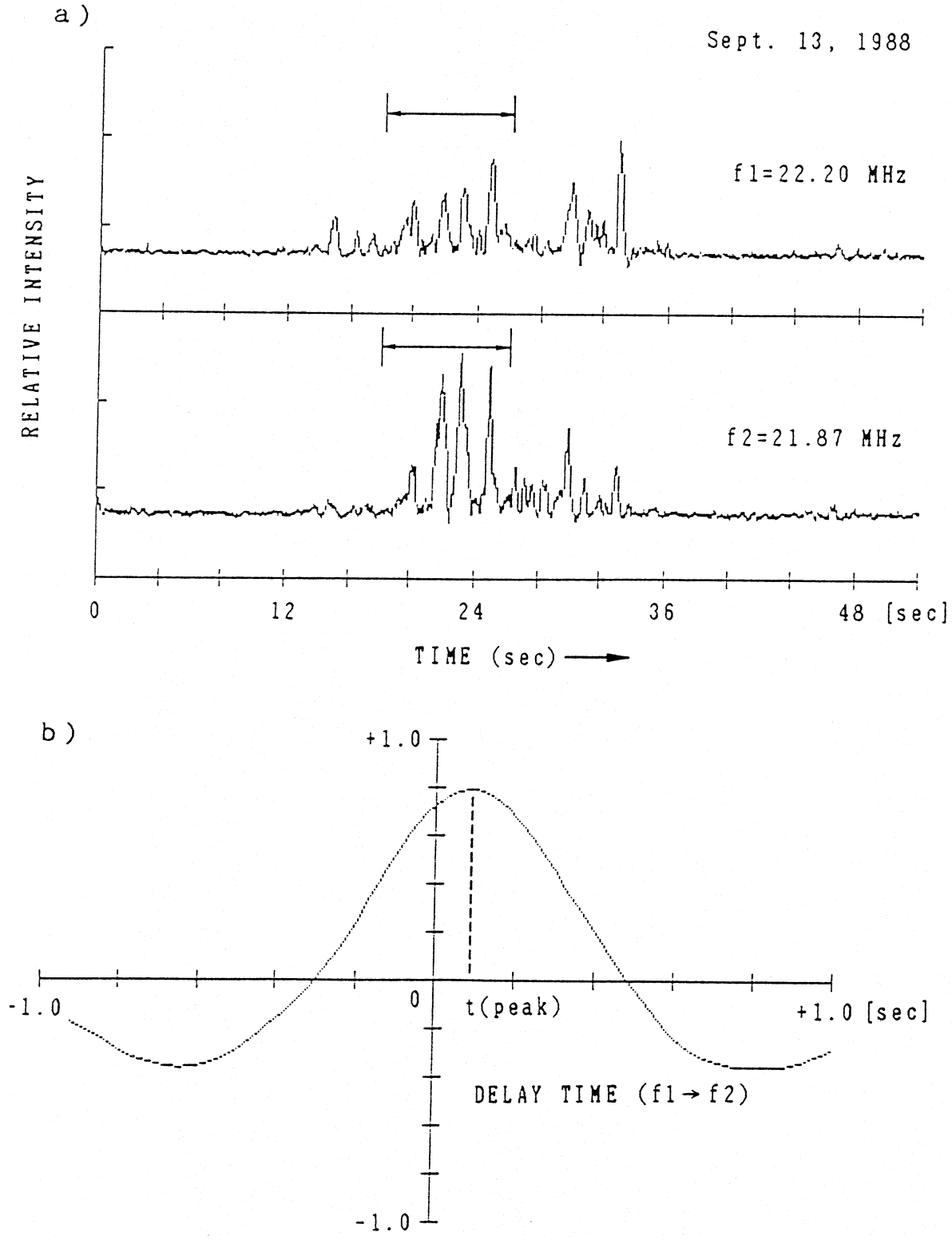

Figure 2: Cross–correlation analysis. The cross–correlation analysis was made for each pair of the selected data segments (as shown by the arrows in the upper panel), and the delay time at the peak correlation, t(peak), was estimated.

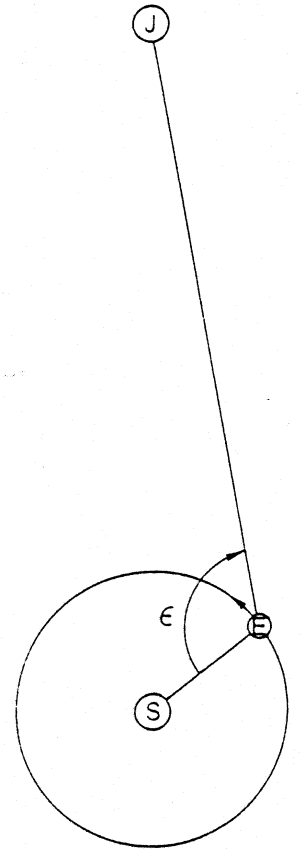

Figure 3: Definition of elongation (ϵ). S, E, and J indicate the sun, Earth, and Jupiter, respectively. The elongation is measured clockwise from 0° to 360° as shown in this figure.

motion of the IPS diffraction pattern would have been smaller than that of the orbital motion of Earth, although both motions occurred in approximately the same direction.

Figure 5 shows the result for an Io–B storm that occurred after opposition ($\epsilon = 225°$). As seen in Figure 5, the negative frequency drift was dominant for the Io–B storm after opposition, being opposite to the sense of the frequency drift for the Io–A storm.

We calculated the average delay time for each Io–A storm, and the average frequency drift rate between the two frequencies at which we had observed was estimated by dividing the frequency difference by the average delay time. In Figure 6, the estimated average frequency drift rates are plotted as a function of elongation. As seen in Figure 6, the frequency drift rate changes systematically as a function of elongation.

The dashed curve in Figure 6 is a simulated one based on a simple IPS model. We assumed in the model that the screen causing IPS is concentrated and located at a distance of 0.2 AU from Earth in the line of sight, and moving radially outward from the sun with a constant velocity. We also assumed that the emission source geometry as projected on the sky plane is approximately the same for a given storm component (i.e., Io–A storm in this case). In such a model the relative variation of the IPS frequency drift rate is determined by the solar–wind velocity component perpendicular to the line of sight at the screen, and the orbital velocity component of Earth perpendicular to the line of sight. We calculated the relative variation of the frequency drift rate by the model and obtained the best–fit curve by assuming that the frequency drift rate at $\epsilon = 90°$ is -5 MHz sec^{-1}. Changing the assumed screen distance from Earth did not significantly change the shape of the relative–variation curve. The calculated curve of the IPS frequency drift rate variation fits relatively well with the estimated points as seen in Figure 6. In a future

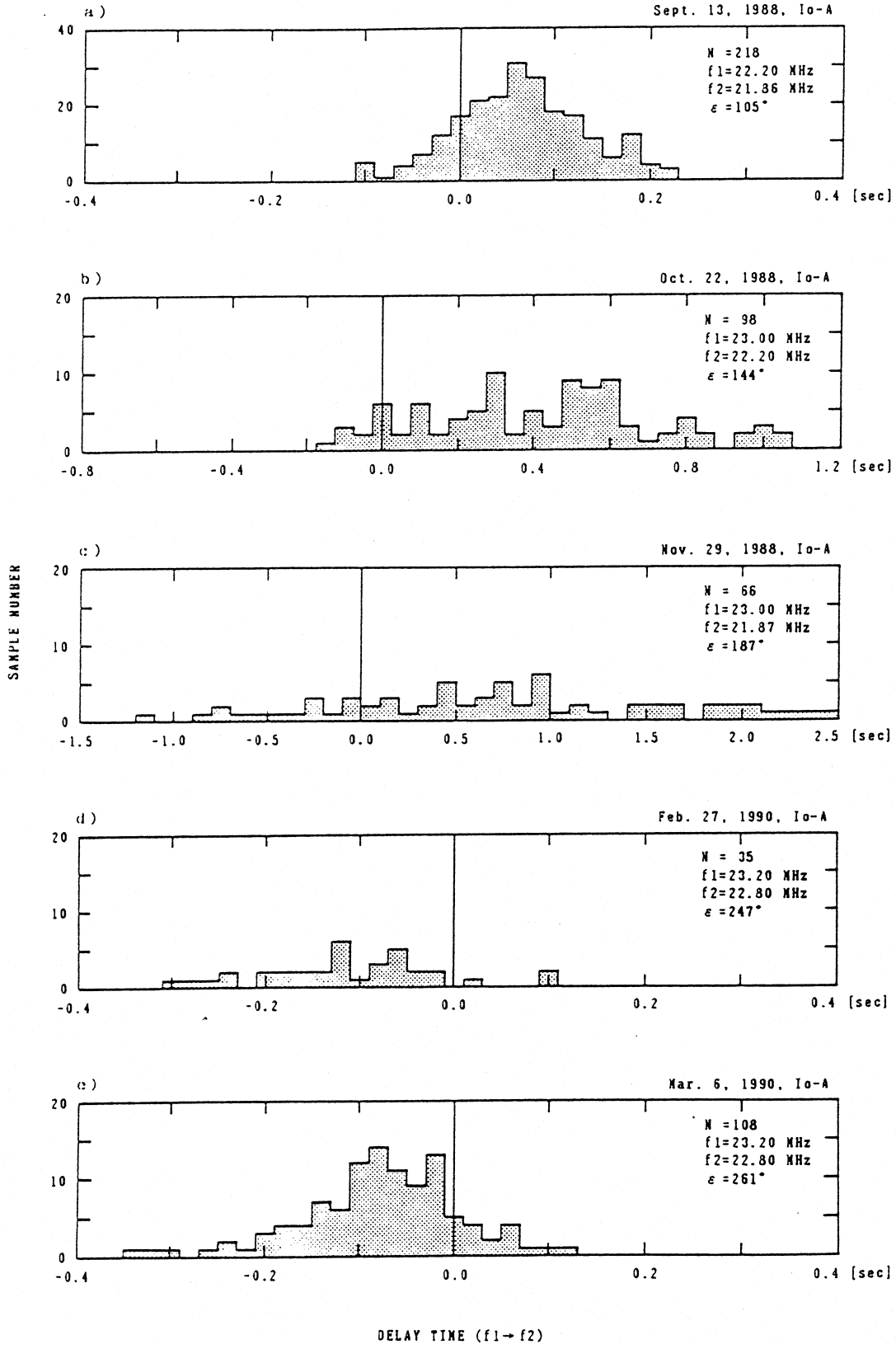

Figure 4: Delay–time distribution diagrams for the 5 Io–A storms. N and ϵ indicate the total sample number, and the elongation for the corresponding storm, respectively. Two frequencies (f1 and f2) at which we observed are also indicated in each panel.

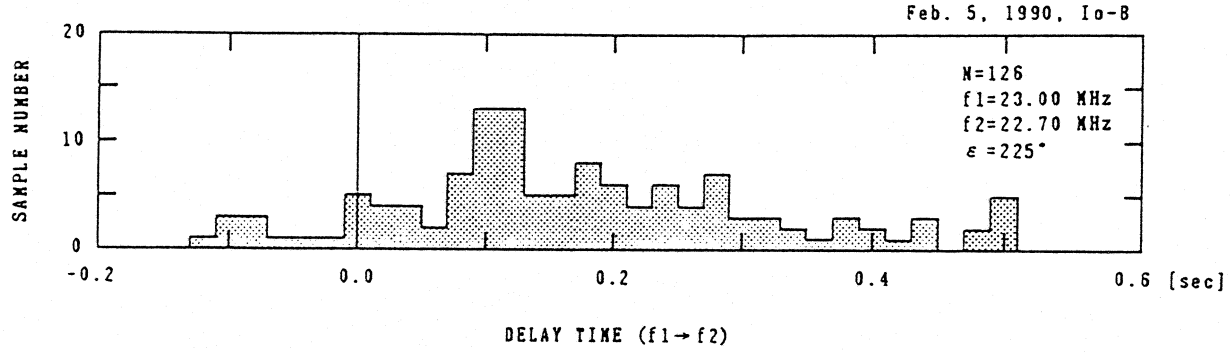

Figure 5: Delay–time distribution for an Io–B storm that occurred after opposition.

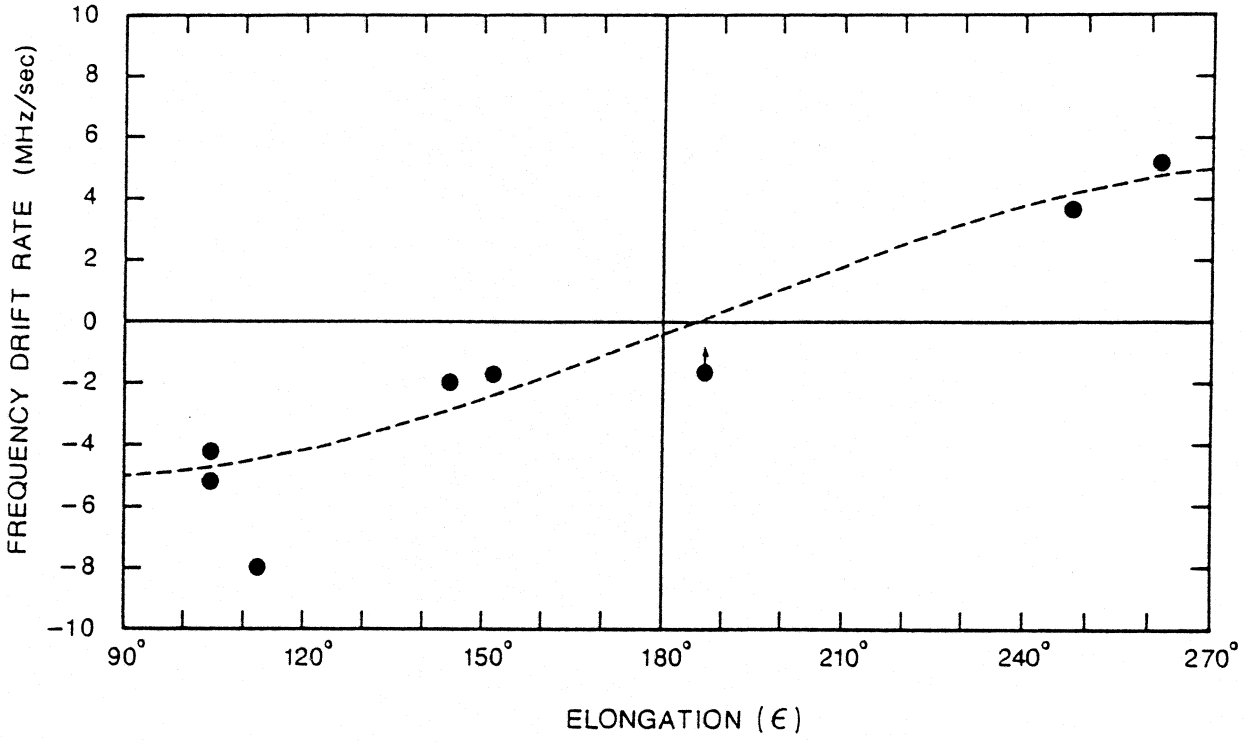

Figure 6: Variation of the IPS frequency drift rate for the Io–A emission as a function of elongation. The estimated point with the arrow should be closer to the horizontal axis of a frequency drift rate of 0 MHz sec^{-1}. The dashed curve is a theoretically derived one based on a simple IPS model (see text).

analysis, we will refine the IPS model by taking account of the distribution of the electron density irregularities and solar wind velocity along the line of sight.

6 Conclusions

We confirmed, based on the two–frequency observations at frequencies between 21.8 and 23.3 MHz, the existence of the frequency drift due to the combined effect of the radiating source structure and IPS. The estimated IPS frequency drift rate for the Io–A storm changes systematically as a function of elongation. The observed frequency drift rate variation for the Io–A storm is fitted by a simple IPS model, which further confirms that the phenomenon is caused by IPS. The magnitude of the IPS frequency drift rate of the Io–A storm at an elongation of 90° is estimated to be about 5 MHz sec^{-1} at frequencies of about 22–23 MHz. The sense of the IPS frequency drift of the Io–A storm is opposite to that of the Io–B storm.

Acknowledgments: I wish to express my thanks to Dr. T. D. Carr, University of Florida, for reading the manuscript.

References

Boischot, A., J.H. Sastri, and P. Zarka, Localization of Io and non–Io sources of Jovian decameter emission, *Astron. Astrophys.*, **175**, 287, 1987.

Carr, T. D., M.D. Desch, and J.K. Alexander, Phenomenology of magnetospheric radio emissions, in *Physics of the Jovian Magnetosphere, edited by A.J. Dessler*, p.226, Cambridge Univ. Press, New York, 1983.

Douglas, J.N. and H.J. Smith, Interplanetary scintillation in Jovian decametric radiation, *Astrophys. J.*, **148**, 885, 1967.

Genova, F., and A. Boischot, Structure of the source of Jovian decametric emission and interplanetary scintillation, *Nature*, **293**, 382, 1981.

Genova, F., and Y. Leblanc, Interplanetary scintillation and Jovian DAM emission, *Astron. Astrophys.*, **98**, 133, 1981.

Goldstein, M. L., and C.K. Goertz, Theories of radio emissions and plasma waves, in *Physics of the Jovian Magnetosphere, edited by A.J. Dessler*, p.317, Cambridge Univ. Press, New York, 1983.

Maeda, K., Interplanetary scintillation in Jupiter's decametric radiation, *Publ. Astron. Soc. Japan*, **33**, 465, 1981.

Maeda, K, Broadband observations of Jovian decametric radiation, *Solar Terrest. Environ. Res. Japan*, **11**, 14, 1987.

Slee, O.B., and C.S. Higgins, The solar wind and Jovian decameter radio emission, *Austral. J. Phys.*, **21**, 341, 1968.